

NJC

Accepted Manuscript



This is an *Accepted Manuscript*, which has been through the Royal Society of Chemistry peer review process and has been accepted for publication.

Accepted Manuscripts are published online shortly after acceptance, before technical editing, formatting and proof reading. Using this free service, authors can make their results available to the community, in citable form, before we publish the edited article. We will replace this *Accepted Manuscript* with the edited and formatted *Advance Article* as soon as it is available.

You can find more information about *Accepted Manuscripts* in the [Information for Authors](#).

Please note that technical editing may introduce minor changes to the text and/or graphics, which may alter content. The journal's standard [Terms & Conditions](#) and the [Ethical guidelines](#) still apply. In no event shall the Royal Society of Chemistry be held responsible for any errors or omissions in this *Accepted Manuscript* or any consequences arising from the use of any information it contains.

**Preparation and characterization of Ti supported bimodal mesoporous catalysts
using a self-assembly route combined with a ship-in-a-bottle method**

Shiyang Bai, Xintao Hu, Jihong Sun*, Bo Ren

Corresponding author: Jihong Sun

Detailed permanent address:

Department of Chemistry and Chemical Engineering

College of Environmental & Energy Engineering

Beijing University of Technology

100 PingLeYuan, Chaoyang District

Beijing, 100124, P. R. China

E-mail address: jhsun@bjut.edu.cn

Tel.: +86-010-67396118

Fax: +86-010-67391983

**Preparation and characterization of Ti supported bimodal mesoporous catalysts
using a self-assembly route combined with a ship-in-a-bottle method**

Shiyang Bai, Xintao Hu, Jihong Sun*, Bo Ren

College of Environmental & Energy Engineering, Beijing University of Technology,

Beijing 100124, P. R. China

Abstract: Ti/BMMs (bimodal mesoporous silica) catalysts have been prepared via a self-assembly route combined with a ship-in-bottle technique. Four different methods were carried out to investigate the effects of adding ionic liquid [spmim][Cl⁻] (1-methyl-3-(3-trimethoxysilane) propylimidazole chloride) and triethanolamine (TEAOH) or triethylamine (TEA) on the coordination environment of the titanium species in the mesopores. The structure characteristic and texture properties of resultant samples were characterized by XRD, FT-IR, N₂ adsorption-desorption isotherms, TGA, and UV-Vis spectra. The results showed that the bimodal mesoporous structure of Ti/BMMs could be preserved after grafted Ti species via four preparation methods. On the other hand, the presence of [spmim][Cl⁻] and TEAOH or TEA could not only prevent titanium species existing in the mesoporous surface from aggregation, but also benefit for loaded tetrahedrally-coordinated titanium species with a high dispersion. Finally, their catalytic activities by the epoxidation of cyclohexene preliminarily indicated that the influence of Ti loading methods on the conversion of cyclohexene was remarkable.

Key words: Bimodal mesoporous silicas; ionic liquid; Ti/BMMs; epoxidation of cyclohexene

1. Introduction

In the past decade, Titanium-substituted zeolites have received great attention due to their excellent catalytic properties in selective oxidation reactions under mild conditions. Microporous

zeolites such as TS-1 [1], Ti-Beta [2] and Ti-MWW [3, 4] are widely used as commercial catalysts, but their micropores easily hinder the access of bulky substrates as well as of large organic hydroperoxides. Nowadays, in the fine chemical and pharmaceutical industries, the bulky reactants are very common [5, 6], and therefore, how to prepare novel titanosilicates with larger pores has attracted much attention. Presently, several titanium-containing mesoporous materials, such as Ti-MCM-41 [7, 8], Ti-HMS [9], Ti-MCM-48 [10], and Ti-SBA-15 [11, 12] have been systemically investigated by incorporating titanium ions into the framework site of substituted mesopores via one-pot routes using a co-condensation pathway or post-synthesis methods through functional modification. However, a significant fraction of the tetrahedrally-coordinated titanium species lie buried inaccessibly in the mesoporous framework. To overcome these drawbacks, Maschmeyer et al. [13] obtained a mesoporous Ti/MCM-41 material with high catalytic performances in epoxidation reactions by grafting titanocene onto the inner surface of mesoporous silica MCM-41, subsequently, the research results showed that the presence of surface water in the one-dimensional channels may lead to the formation of hydroxy-bridged dimers and higher oligomers [14]. Shan et al. [15] synthesized titanosilica molecular sieves Ti-TUD-1 with three-dimensional randomly connected mesopores, and the resultant catalysts possessed high activity for cyclohexene epoxidation. All of the research conclusions mentioned above indicated that by choosing a suitable synthesis method and controlling the coordination of titanium species, the mesoporous titanosilicas with an excellent catalytic performance could be created. However, the one-dimensional mesoporous structure of traditional mesoporous molecular sieves would still obstruct the diffusion behaviours and reaction properties of large molecules, which strongly influence the catalytic performances of selective epoxidation.

Recently, some reports demonstrated that the mesoporous materials with hierarchical interconnecting three-dimensional pore networks have obvious advantages as supports, which provide easier accessibility for larger reactant molecules to the active site and thereby improve reaction efficiencies [16, 17, 18]. For example, the bimodal mesoporous materials (BMMs) [16] possess a bimodal mesoporous structure with independently-controlled small pores (~3 nm) and large pores (in the range of 15-50 nm), as well as abundant silanol groups on the mesoporous surface. Compared with traditional mesoporous M41s with a single pore distribution, the unique bimodal mesoporous structures of BMMs could provide the larger molecules easier access to the active site due to the disappearance of diffused limitation, as well as reducing the accumulation of reactants and products, and thereby improving the reaction efficiency. At present, our group has grafted Ti species onto the mesoporous surface of BMMs using a post-synthesis method [17], and the catalytic performances of obtained Ti/BMMs were tested by epoxidation of cyclohexene, which showed a higher selectivity, but, rapid deactivities. The main reason is the leaching of tetrahedrally-coordinated titanium species existing in the mesoporous surface of BMMs. Thus, the aim of this work is to investigate the maintenance of good catalytic properties by stabilizing the active species inside the mesoporous channels.

Herein, combining with the ship-in-a-bottle technique based on our previous work, we report post-synthesis procedures of Ti-doped BMMs with titanocene dichloride as titanium source through a post-treatment via self-assemble route of ionic liquid [spmim][Cl]. Meanwhile, in order to realize the high dispersion of tetrahedrally-coordinated titanium species on the mesoporous surface of BMMs, triethanolamine or triethylamine was used to control the coordination of titanium species. In addition, the Ti/BMMs catalysts were characterized by means of X-ray

diffraction (XRD), Fourier Transform Infrared Spectroscopy (FT-IR) spectra, N₂ adsorption-desorption techniques, Thermogravimetric analysis (TGA), and UV visible spectroscopy (UV-vis). Furthermore, the preliminary catalytic performance of the catalysts was investigated by the epoxidation of cyclohexene.

2. Experimental

2.1 Chemicals

The chemicals used in this work including cetyltrimethylammonium bromide (CTAB), ethyl silicate (TEOS), ammonium hydroxide, triethanolamine, triethylamine, ether, dichloromethane and chloroform were obtained from Beijing Chemical Works. Besides, cyclohexene, 3-chloropropyltrimethoxysilane (97 %), 1-methylimidazole (99 %), tert-butyl hydroperoxide (TBPH) and titanocene dichloride (Cp₂TiCl₂) were supplied by Alfa Aesar Company. All the chemicals were all A. R. grade.

2.2 Synthesis of Catalyst

2.2.1 Synthesis of ionic liquid [spmim][Cl⁻]

8 ml of 3-chloropropyltrimethoxysilane and 4 ml of 1-methylimidazole were added into a glass flask, and then mixture was kept stirring and refluxing at 95 °C under N₂ atmosphere. The molar ratio of 3-chloropropyltrimethoxysilane to 1-methylimidazole was about 0.87. After reacting for 24 h, the white mixture gradually changed into a brown viscous liquid, and subsequently washed with ether, and dried under vacuum conditions at 60 °C for 3 h. Finally, the ionic liquid [spmim][Cl⁻] was obtained and denoted as IL.

2.2.2 Grafting IL onto the surface of BMMS

BMMS was synthesized partially based on the literature method [16]. In a typical process,

CTAB (2.6115 g) was dissolved completely in water (104 mL) to get a transparent solution. 8 ml of TEOS was added to the solution while stirring. Finally, ammonium hydroxide was added quickly to adjust pH to around 9. The mixture was stirred continuously to get a white gel. The molar composition of the synthesis gel was as follow: CTAB: TEOS: H₂O: NH₃ = 1: 4.97: 814.7: 4.72. The resultant precipitates were filtered, washed, and dried at 120 °C for 3 h. To remove surfactant, the solid was calcined at 550 °C for 6 h, with a heating rate of 5 °C/min from room temperature to 550 °C.

Prior to the grafting process, BMMs were outgassed under vacuum conditions at 150 °C for 3 h. In a distillation apparatus, 0.5 g of IL were dissolved in 10 mL of chloroform, and treated with 1 g of previously prepared BMMs. Then the mixture was kept stirring and refluxing at 60 °C under N₂ atmosphere. After reacting for 24 h, the obtained mixture was filtered, washed with dichloromethane, dried under high vacuum at 60 °C for 3 h. Thus, the IL grafted BMMs was obtained and denoted as ILBMMs (the molar ratio of IL with BMMs was around 0.1).

2.2.3 Preparation of Ti/BMMs catalyst

Method 1: 0.03 g of Cp₂TiCl₂ were dried under vacuum conditions at 120 °C for 1 h, and then cooled down under N₂ atmosphere. The dried Cp₂TiCl₂ were dissolved in 5 mL of chloroform and then 0.5 g of BMMs, 1.7 mL of triethylamine and 0.25 g IL were added. After stirring at room temperature under a dry N₂ atmosphere for 8 h, the obtained mixture was filtered, washed with dichloromethane, dried at 60 °C under high vacuum for 3 h. To remove IL, the solid was calcined at 450 °C for 6 h and the sample was marked as Ti/BMMs-1.

Method 2: This method was almost same as Method 1, except that the triethylamine was substituted with triethanolamine. The corresponding obtained sample was marked as Ti/BMMs-2.

Method 3: 0.03 g of Cp₂TiCl₂ were dried under vacuum at 120 °C for 1 h, and then cooled down under N₂ atmosphere. The dried Cp₂TiCl₂ were dissolved in 5 mL of chloroform and then 0.65 g of ILBMMs and 1.7 mL of triethylamine were added. After stirring at room temperature

under a dry N₂ atmosphere for 8 h, the obtained mixture was filtered, washed with dichloromethane, dried at 60 °C under high vacuum for 3 h. To remove IL, the solid was calcined at 450 °C for 6 h and the sample was marked as Ti/BMMs-3.

Method 4: This method was almost same as Method 3, except that the triethylamine was substituted with triethanolamine. The resultant sample was marked as Ti/BMMs-4.

The Ti loading amount was around 0.89 % (wt) for Ti/BMMs-1, and -2; however, was about 1.65 % (wt) for Ti/BMMs-3, and -4.

2.2.4 Catalytic test

The epoxidation of cyclohexene with TBHP was carried out in a three necked flask equipped with a condenser under vigorous stirring which was heated with an oil bath. TBHP was dried using anhydrous MgSO₄ before use. Typically, 100 mg of catalyst, 10 mL of chloroform as solvent, 10 mmol of cyclohexene, 11 mmol of TBHP and 5 mmol of mesitylene (internal standard) were mixed in the flask and heated to 60 °C under a dry nitrogen atmosphere. The reaction products were withdrawn at different sampling times and analyzed by gas chromatography (GC-7890□, TIANMEI) equipped with a flame ionization detector, using a HP-5MS capillary column. After the reaction for 6 h, the powder was removed from the reaction mixture by filtration. Epoxide selectivity was related to the cyclohexene converted according to the following equation:

$$S(\%) = 100 \times \frac{[\text{Epoxide}]}{[\text{Cyclohexene}]_0 - [\text{Cyclohexene}]}$$

where epoxide represents cyclohexene oxide, the subscript 0 stands for initial values, and all concentrations are expressed on a molar basis.

2.3 Characterization

The powder XRD measurements were recorded using a BEIJING PERSEE XD-3 X-ray diffractometer using CuK_α radiation (λ=0.154056 nm) source for 2θ ranging from 0.6 ° to 10.0 ° with a scanning speed of 0.02°/s at 36 KV and 20 mA. FT-IR spectra were observed on a Bruker TENSOR-27 analyzer with KBr pellet. N₂ adsorption and desorption isotherms at -196 °C were obtained using a Micromeritics Tristar II. Before nitrogen adsorption, the samples were pretreated

for 5 h under helium at 100 °C. The isotherm data were analyzed with BET (Brunauer-Emmett-Teller) and the plots of the corresponding pore size distribution were obtained from desorption branches of the isotherms by using BJH (Barrett-Joyner-Halenda) model. The TGA were carried out between 25 and 800 °C using a Perkin-Elmer Pyris 1 TG analyzer under 20 mL/min N₂ flow with a heating rate of 10 °C/min. UV-vis spectra were recorded on a SHIMADZU UV-2450 spectrophotometer. The Ti amount was determined by ICP-AES (Optima 2000DV).

3. Results and Discussion

3.1 XRD analysis

(Insert Figure 1)

Figure 1 shows the XRD patterns of BMMs (a), ILBMMs (b) and Ti/BMMs-(1~4) (c-f). As can be seen, the XRD pattern of BMMs (Figure 1a) clearly exhibited (100) a diffraction peak at $2\theta = 2.11^\circ$, and the corresponding value of the d space was around 4.18 nm, which was consistent with that of reported reference [16]. After grafting IL, the (100) peak intensity of ILBMMs (Figure 1b) decreased and its 2θ position shifted to 2.17° (corresponding value of d space decreased to 4.07 nm), indicating that the interaction between the IL and the superficial silanol groups of BMMs resulted in the disruptiveness of the mesostructures, and the decrease of d -spacing was properly due to the structural shrinkage during the grafting process. As for the XRD patterns of synthesized Ti/BMMs with different methods (Figure 1c-f), the (100) diffraction peak could still be observed at a higher position of 2θ around 2.30° , whereas the d space value corresponded to 3.77 nm. Besides that, the peak (100) intensity decreased obviously with the comparison of pure BMMs (Figure 1a) and ILBMMs (Figure 1b), suggesting that the influence of introduction of Ti species onto the surface of BMMs on the mesopore ordered degree was obvious.

3.2 FT-IR analysis

The FT-IR spectra of related samples are depicted in Figure 2 and Figure S1 (see Supplementary Information). For IL (Figure 2a), the absorption bands at 1573 cm^{-1} and 1458 cm^{-1} were attributed to the C=C symmetrical stretching vibration, while the bands at 810 cm^{-1} corresponded to bending vibrations of the imidazole ring. Besides, the bands at 2842 cm^{-1} , 2950 cm^{-1} and 1184 cm^{-1} were ascribed to the C-H and C=N stretching vibrations, respectively. All of these absorptions belonged to the characteristic bands of IL, which were also presented in the FT-IR spectra of the Ti/ILBMMs samples (before calcination for Ti/BMMs) in Figure S1. As for BMMs (Figure 2b), the bands at 1085 cm^{-1} , 960 cm^{-1} and 815 cm^{-1} were attributed to the asymmetric stretching vibrations, symmetrical stretching vibrations and bending vibrations of the mesoporous framework (Si-O-Si), respectively. It is worth pointing out that the band at 960 cm^{-1} in Figure 2d-g also can be attributed to the symmetrical stretching vibrations of Si-O-Ti [20]. Additionally, Figure 2c presents the FT-IR spectrum of ILBMMs, as can be seen, the appearance of new bands can be assigned to the C-H and C=N vibrations of imidazole rings, which further confirms the successful grafting of IL onto the mesopore surface of BMMs [19-21]. Although these observations cannot be used as the direct evidence of the introduction of Ti, all disappearances of the stretching vibration characteristic peaks of C-H bonds for Ti/BMMs samples (Figure 2d-g) implied the complete removal of organic groups after calcination at $450\text{ }^{\circ}\text{C}$.

(Insert Figure 2)

3.3 N₂-sorption analysis

N₂ adsorption-desorption isotherms and corresponding pore size distributions of samples are shown in Figure 3 and Table 1. All of the samples exhibited the type IV isotherms and the

characteristics of the mesoporous systems [22]. As can be seen in Figure 3a, the isotherms of BMMs showed two inflections: the first occurs at $0.30 < P/P_0 < 0.40$ and the second at $0.75 < P/P_0 < 0.95$, along with the corresponding pore size distribution (inserted in Figure 3), proving the existence of the two mesopore distributions with a narrow small pore distribution around 2.79 nm and a large pore distribution around 21.02 nm, respectively. In addition, the BET specific surface area and pore volume of BMMs were $980 \text{ m}^2/\text{g}$ and $1.85 \text{ cm}^3/\text{g}$, respectively. After grafting IL onto the surface of BMMs (Figure 3b), the two inflections both moved to the lower relative pressure, and the small and large mean pore size decreased to 2.15 nm and 19.69 nm, respectively. Meanwhile, the BET surface area and pore volume also shrunk to $601 \text{ m}^2/\text{g}$ and $1.07 \text{ cm}^3/\text{g}$, verifying the appearance of IL inside the channels of BMMs.

(Insert Figure 3 and Table 1)

In order to explore the influence of Ti species on the mesostructure of BMMs, Ti/BMMs-3 was taken as an example to be characterized with N_2 -sorption isotherm (Figure 3c). It is obvious that the texture parameters of Ti/BMMs-3 were all smaller than that of BMMs, including the small and large mean pore size (2.64 nm and 19.85 nm), surface area ($876 \text{ m}^2/\text{g}$) and pore volume ($1.46 \text{ cm}^3/\text{g}$), suggesting that the Ti species might occupy the inner mesoporous space of BMMs [23]. However, compared with that of ILBMMs (Figure 3b), the texture parameters of Ti/BMMs-3 including the increased pore size, larger surface area and pore volume were ascribed to the decomposition and removal of IL inside the mesoporous channels of BMMs.

3.4 TGA performance

(Insert Figure 4)

TGA illustrations of samples at a heating rate of $10 \text{ }^\circ\text{C}/\text{min}$ are presented in Figure 4. For

BMMs (Figure 4a), the weight loss between 30-100 °C was attributed to the physisorbed water, and another in the temperature range of 100-500 °C was appointed to dehydration of water on silanol groups. While the weight losses at 500-800 °C was attributed to the condensation of silanol groups. The total weight loss of BMMs was around 7.2 %wt. As for ILBMMs (Figure 4b), these two obvious weight losses in the temperature range of 223-365 °C and 365-600 °C were assigned to the decomposition of IL grafted on the surface of BMMs [24], presumably suggesting that IL loading amount was around 18 %wt. Besides, the TGA curve of Ti/BMMs-3 (Figure 4c) exhibited two weight loss processes: the first one between 30-100 °C belonged to the desorption of physisorbed water, while the second one after 100 °C was corresponding to the dehydration of silanols. However, it is very noticeable that the total weight loss of Ti/BMMs-3 was much lower than that of BMMs, indicating the substitution of superficial Si-OH groups with Ti on the inner surface of BMMs.

3.5 UV-vis analysis

(Insert Figure 5)

The positive imidazole ring of IL possesses six electrons, which obeys the Hückel's $4n+2$ rule, and therefore the imidazole ring has aromatic properties. The UV spectra of samples are presented in Figure 5. As can be seen, the UV absorption peaks of IL (Figure 5b), ILBMMs (Figure 5c) and Ti/ILBMMs (Figure S2) were both at $\lambda_{\max}=216.8$ nm, corresponding to the positive imidazole ring. In contrast, there was no absorption for pure BMMs (Figure 5a and Figure S2) at the same position. These results indicate the successful grafting of IL onto the surface of BMMs.

Besides, with the help of UV-vis spectra, the coordination environment of Ti species would

be demonstrated [25, 26]. Figure 5(insert) and Figure 2S show the diffusion reflectance UV-vis spectra of four Ti/BMMs samples, Ti/ILBMMs and mixture of Cp_2TiCl_2 with BMMs. These observations obviously indicate a strong interaction between IL and Cp_2TiCl_2 , although the coordination environment of Ti species is still unclear, which is very important and also reminds us to study in depth in the following investigates. However, it can be seen that the absorption bands of all samples of Ti/BMMs were at the wavelength range of 210 and 240 nm, which could be ascribed to the electronic transition from the $2p$ bonding orbital of oxygen to the d orbital of tetrahedrally-coordinated Ti-sites, suggesting that most of the titanium species existing on the external surface of BMMs are tetrahedrally-coordinated [27]. Meanwhile, for a Ti/BMMs-1 sample (Figure 5d), a wide absorption band around 260 nm could be attributed to the hexacoordinate titanium species [28], suggesting the appearance of TiO_2 -like microclusters. On the other hand, for Ti/BMMs-2 (Figure 5e), Ti/BMMs-3 (Figure 5f) and Ti/BMMs-4(Figure 5g), the absorption bands between 240 nm and 320 nm were not observed, meaning a less hexacoordinated titanium species. Particularly, the UV absorption band of Ti/BMMs-4 (Figure 5g) was at 222.4 nm, while the bands of other samples (Ti/BMMs-1, Ti/BMMs-2 and Ti/BMMs-3, as depicted in Figure 5d-f) were at 226.3 nm. Hence, it can be concluded that the titanium environment of Ti/BMMs-4 is similar to that of TS-1 [29, 30], suggesting the high dispersion of tetrahedrally-coordinated titanium species on the surface of Ti/BMMs-4.

(Insert Scheme 1A and 1B)

Based on the characterization results discussed above, it can be deduced that the synthesis parameters have a great influence on the anchored amount and titanium-coordinated environments. According to the synthesis route (method 1 and method 2), it would be difficult for the resultant

large complex molecules derived from Cp_2TiCl_2 , triethanolamine or triethylamine and IL molecules to diffuse into the mesoporous channels of BMMs, which led to the poor dispersion and low amount of Ti-loading. Comparably, in accordance with synthesis route (method 3 and method 4), using the ship-in-a-bottle method, IL were grafted onto the surface of BMMs with a uniform dispersion, and then, the resultant small complex molecules stemmed from Cp_2TiCl_2 , and triethanolamine or triethylamine would be steadily anchored into the surface of ILBMMs due to the assembly interaction of superficial IL and Cp_2TiCl_2 . The detailed schematic illustrations are presented in scheme 1A and B. However, the relationship between structure properties of mesoporous BMMs and Ti species of tetrahedral-coordinations need to be further investigated.

3.6 Catalytic performances of Ti/BMMs catalysts

(Insert Figure 6)

The catalytic performances of Ti/BMMs catalysts prepared by four different methods with TBHP as oxidant are shown in Figure 6. Overall, it was found that both the conversion of cyclohexene (seen in Figure 6A) and selectivity of cyclohexene oxide (shown in Figure 6B) revealed the increasing tendency with the reaction time extending. Meanwhile, the catalytic activities under the same reaction conditions (Si/Ti molar ratio is around 50) increase according to the following order: Ti/BMMs-4 > Ti/BMMs-3 > Ti/BMMs-2 > Ti/BMMs-1. As can be seen in Figure 6A, taking the reaction time of 6 h as an example, the conversion of cyclohexene was 48 % for Ti/BMMs-1, 57 % for Ti/BMMs-2, 67 % for Ti/BMMs-3, and 70 % for Ti/BMMs-4, while, as depicted in Figure 6B, the selectivity of cyclohexene oxide increased from 66 % for Ti/BMMs-1, to 70 % for Ti/BMMs-2, 79 % for Ti/BMMs-3, and 86 % for Ti/BMMs-4. It should be emphasised that the selectivity of cyclohexene oxide is more important than conversion in this

reaction, obviously, the preparation methods could extensively influence the catalytic performances of Ti/BMMs catalysts on the basis of the following mentioned-above characterization results. Practically, Ti/BMMs-4 catalysts exhibited not only a high conversion (about 70 %) but also a high selectivity (up to 86 %). The main reason is related to the dispersion behaviors of tetrahedrally-coordinated Ti species existing inside the mesoporous surface. For Ti/BMMs-2 and Ti/BMMs-1 prepared as illustrated in Scheme 1A, the resultant large complex molecules derived from Cp_2TiCl_2 , and triethanolamine (or) triethylamine, as well as IL molecules, can hardly diffuse into the mesoporous channels of BMMs, which leads to the poor dispersion and even low loading of Ti species on the mesoporous surface. Comparably, for Ti/BMMs-3 and Ti/BMMs-4 obtained via the ship-in-a-bottle method as demonstrated in Scheme 1B, the grafting of IL onto the surface of BMMs is in favor of the highly uniform dispersions of tetrahedrally-coordinated Ti species, which could play an important role in preventing the aggregation of Ti-contained complexes. Additionally, combined with the results of the UV-vis analysis in Figure 5, it can be deduced that the preparation parameter of adding IL is a critical factor for the coordination environment of Ti species. Furthermore, Ti/BMMs-2 and Ti/BMMs-4 presented higher activity than Ti/BMMs and Ti/BMM-3 respectively, suggesting the effect of amine species in the catalyst synthesis mixture. According to the reference [31, 32], the chemical environment and aggregation of Ti(IV) species are significantly influenced by different amine species. The triethanolamine can coordinate with Cp_2TiCl_2 to form a compound which would prevent the formation of polymerization water with Cp_2TiCl_2 and lead to well dispersion of Ti in BMMs.

4. Conclusions

In summary, Ti/BMMs bimodal mesoporous catalysts were synthesized using four kinds of ship-in-a-bottle methods accompanied with the assembly interaction of IL and Cp_2TiCl_2 . The four Ti/BMMs samples obtained were characterized with XRD, FT-IR, N_2 adsorption-desorption isotherms, TG analysis, and UV-Vis, and the results demonstrated that the mesostructure and the titanium environment were greatly influenced by the different synthesis methods. Meanwhile, the surface area and the pore volume of obtained Ti/BMMs samples gradually decreased by accompany with introduction of Ti-sites onto the mesoporous surface of BMMs. Particularly, The Ti/BMMs-4 prepared by firstly grafting IL onto the surface of BMMs presented the high dispersions of tetrahedrally-coordinated titanium species in the mesoporous surfaces. The preliminary catalytic results including the conversion of cyclohexene and selectivity of cyclohexene oxide showed that the preparation methods could extensively influence the catalytic performances of Ti/BMMs catalysts.

Supplementary Information:

FT-IR and Uv-vis spectra of Ti/ILBMMs (Ti/BMMs before the calcination) are available free of charge via the Internet.

Acknowledgements

This work was supported by the National Natural Science Foundation of China (21076003, 21272005), and the Funding Project for Academic Human Resources Development in Institutions of Higher Learning under the jurisdiction of the Beijing Municipality (PHR201107104, 005000541211019/20, and 005000543111517).

References

- [1] M. Taramasso, G. Perego and B. Notari, U. S. Patent 4410501, 1983.
- [2] A. Corma, P. Esteve, A. Martinez and S. Valencia, *J. Catal.*, 1995, **152**, 18.

- [3] J. M. Thomas, *Angew. Chem. Int. Ed.*, 1999, **38**, 3588.
- [4] L. L. Wang, Y. M. Liu, W. Xie, H. H. Wu, X. H. Li, M. Y. He and P. Wu, *J. Phys. Chem. C*, 2008, **112**, 6132.
- [5] T. Blasco, A. Corma, M.T. Navarro and J. Pérez-Pariente, *J. Catal.*, 1995, **156**, 65.
- [6] G. W. Huisman and D. Gray, *Curr. Opin. Biotechnol.*, 2002, **13**, 352.
- [7] M. Gil, J. A. Organero, M. T. Navarro, A. Corma, A. Douhal, *J. Phys. Chem. C*, 2012, **116**, 15385.
- [8] K. F. Lin, P. P. Pescarmona, K. Houthoofd, D. D. Liang, G. V. Tendeloo, P. A. Jacobs, *J. Catal.*, 2009, **263**, 75.
- [9] P. T. Tanev, M. Chibwe and T. J. Pinnavaia, *Nature*, 1994, **368**, 321.
- [10] M. Morey, A. Davidson and G. Stucky, *Microporous Mater.*, 1996, **6**, 99.
- [11] C.W. Yoon, K. F. Hirsekorn, M. L. Neidig, X. Z. Yang, T. D. Tilley, *ACS Catal.*, 2001, **1**, 1665.
- [12] S. Wu, Y. Han, Y. C. Zou, J. W. Song, L. Zhao, Y. Di, S. Z. Liu and F. S. Xiao, *Chem. Mater.*, 2004, **16**, 486.
- [13] T. Maschmeyer, F. Rey, G. Sankar and J. M. Thomas, *Nature*, 1995, **378**, 159.
- [14] L. Marchese, E. Gianotti, V. Dellarocca, T. Maschmeyer, F. Rey, S. Coluccia and J. M. Thomas, *Phys. Chem. Chem. Phys.*, 1999, **1**, 585.
- [15] Z. Shan, J. C. Jansen, L. Marchese and T. Maschmeyer, *Micro. Meso. Mater.*, 2001, **48**, 181.
- [16] J. H. Sun, Z. P. Shan, T. Maschmeyer and M.-O. Coppens, *Langmuir*, 2003, **19**, 8395.
- [17] S. M. He, Y. Z. Li, L. H. Zhang, X. Wu and J. H. Sun, *Chinese J. Appl. Chem.*, 2009, **122**, 284.

- [18] S. J. Qiu, J. H. Sun, Y. Z. Li and L. Gao, *Materi. Res. Bull.*, 2011, **46**, 1197.
- [19] Q. Wu, H. Chen, M. H. Han, D. Z. Wang and J. F. Wang, *Ind. Eng. Chem. Res.*, 2007, **46**, 7955.
- [20] M. Guidotti, N. Ravasio, R. Psaro, G. Ferraris and G. Moretti, *J. Catal.*, 2003, **214**, 242.
- [21] G. A. Eimer, S. G. Casuscelli, G. E. Ghione, M. E. Crivello and E. R. Herrero, *Appl. Catal. A: Gen.*, 2006, **298**, 232.
- [22] X. T. Hu, B. Ren, L. Zhang, J. H. Sun, *Acta Petrolei Sinica (Petroleum Processing Section)*, 2012, **28**, 102.
- [23] W. S. Ahn, D. H. Lee, T. J. Kim, J. H. Kim, G. Seo and R. Ryoo, *Appl. Catal. A: Gen.*, 1999, **181**, 39.
- [24] O. C. Vangeli, G. E. Romanos, K. G. Beltsios, D. Fokas, E. P. Kouvelos, K. L. Stefanopoulos and N. K. Kanellopoulos, *J. Phys. Chem. B*, 2010, **114**, 6480.
- [25] B. L. Newalkar, J. Olanrewaju, and S. Komarneni, *Chem. Mater.*, 2001, **13**, 552.
- [26] A. Corma, *Chem. Rev.*, 1997, **97**, 2373.
- [27] S. Klein, B. M. Weckhuysen, J. A. Martens, W. F. Maier and P. A. Jacobs, *J. Catal.*, 1996, **163**, 489.
- [28] A. K. Sinha, S. Seelan, M. Okumura, T. Akita, S. Tsubota and M. Haruta, *J. Phys. Chem. B*, 2005, **109**, 3956.
- [29] M. C. Capel-Sanchez, J. M. Campos-Martin and J. L. G. Fierro, *Appl. Catal. A: Gen.*, 2003, **246**, 69.
- [30] P. Ratnasamy, D. Srinivas and H. Knözinger, *Adv. Catal.*, 2004, **48**, 1.
- [31] M. C. Capel-Sanchez, G. Blanco-Brieva, J. M. Campos-Martin, M. P. de Frutos, W. Wen, J. A.

Rodriguez, J. L. G. Fierro, *Langmuir*, 2009, **25**, 7148.

- [32] E. Gianotti, C. Bisio, L. Marchese, M. Guidotti, N. Ravasio, R. Psaro, S. Coluccia, *J. Phys. Chem. C*, 2007, **111**, 5083.

Lists for Figure and Table captions

Figure 1. XRD patterns of BMMs (a), ILBMMs (b), Ti/BMMs-1(c), -2 (d), -3 (e), -4 (f).

Figure 2. FT-IR spectra of [spmim][Cl⁻] (a), BMMs (b), ILBMMs (c), Ti/BMMs-1 (d), -2 (e), -3 (f), -4(g).

Figure 3. N₂ adsorption/desorption isotherms of BMMs (a), ILBMMs (b), and Ti/BMMs-3 (c), as well as corresponding pore size distributions (insert).

Figure 4. TGA curves of BMMs (a), ILBMMs (b), Ti/BMMs-3 (c).

Figure 5. UV-vis spectra of BMMs (a), [spmim][Cl⁻] (b), and ILBMMs (c), as well as Ti/BMMs-1(d), -2 (e), -3 (f), -4 (g) (insert).

Figure 6. Catalytic performances of (A) conversion of epoxidation of cyclohexene and (B) selectivity of cyclohexene oxide over different Ti/BMMs, (a) Ti/BMMs-1; (b) Ti/BMMs-2; (c) Ti/BMMs-3 and (d) Ti/BMMs-4.

Scheme 1A. Schematic process of Ti/BMMs catalyst preparation (method 1 and method 2).

Scheme 1B. Schematic process of Ti/BMMs catalyst preparation (method 3 and method 4).

Table 1 Structural parameters and textural properties of all samples.

a The total pore volume was determined at the relative pressure of 0.99.

b The mean pore size was calculated from the N₂ desorption branch using the BJH method.

c The results were given by ICP-AES.

d The contents were calculated on the basis of obtained TGA profiles.

Figure 1.

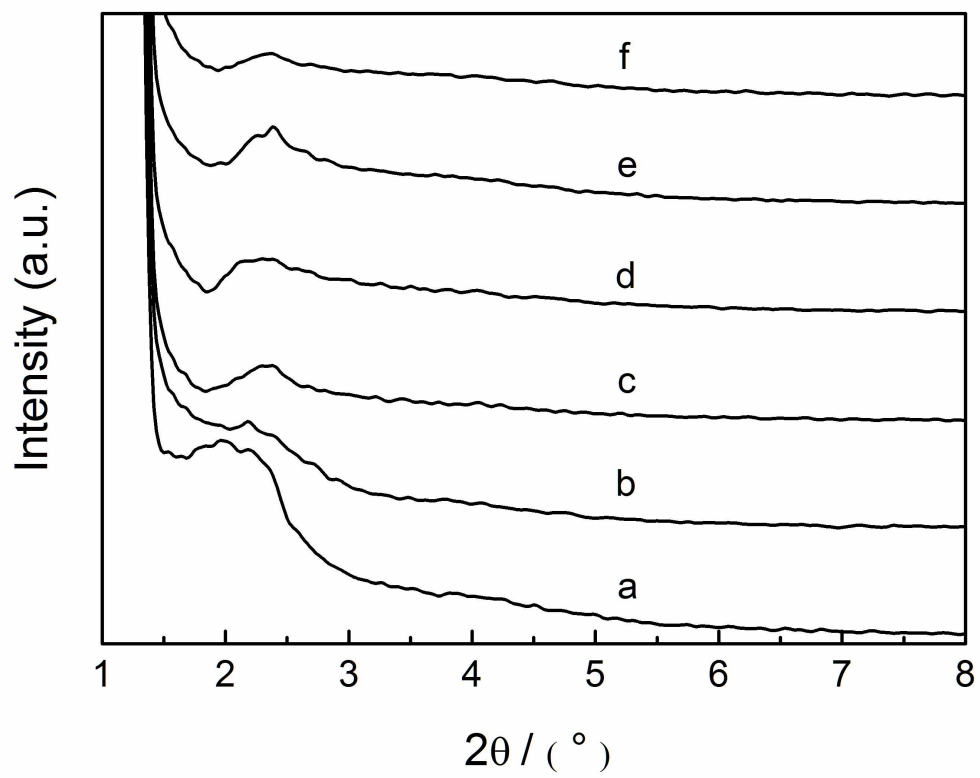


Figure 2.

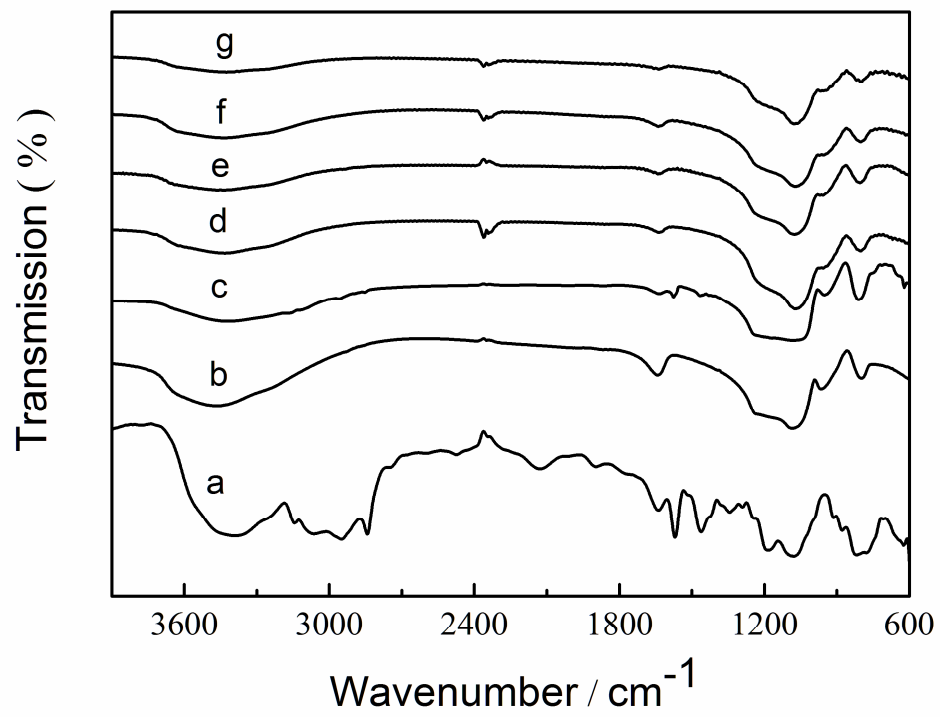


Figure 3.

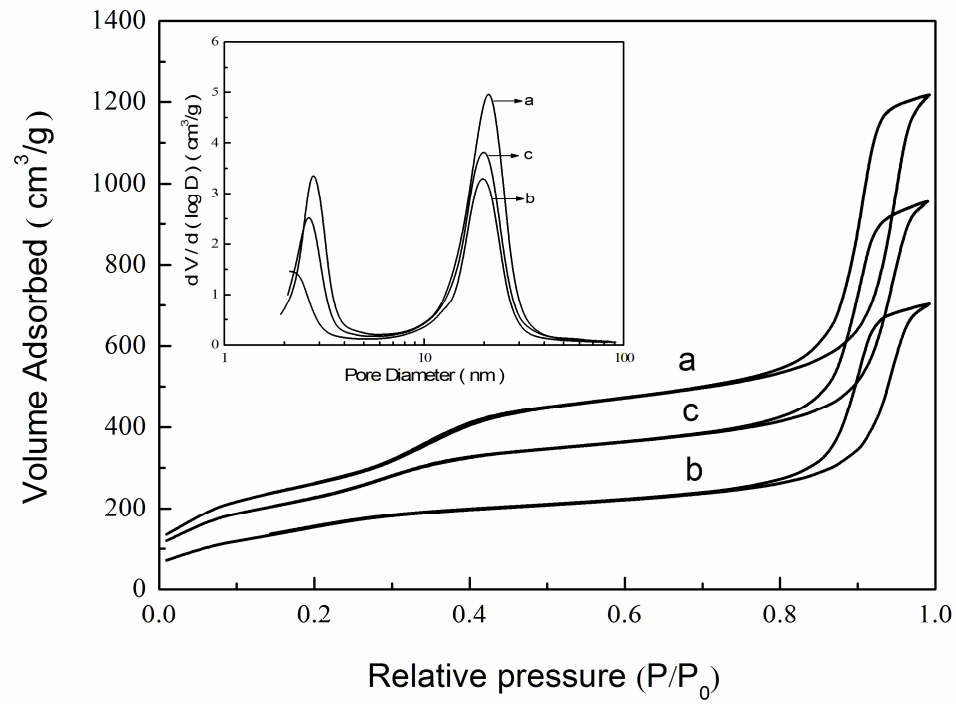


Figure 4.

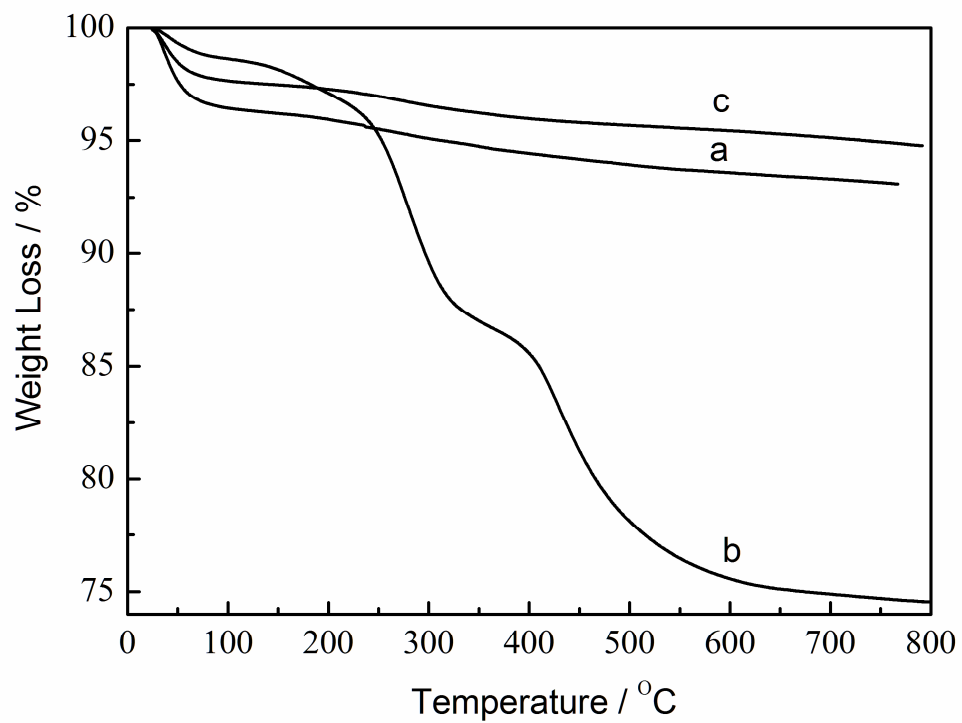


Figure 5.

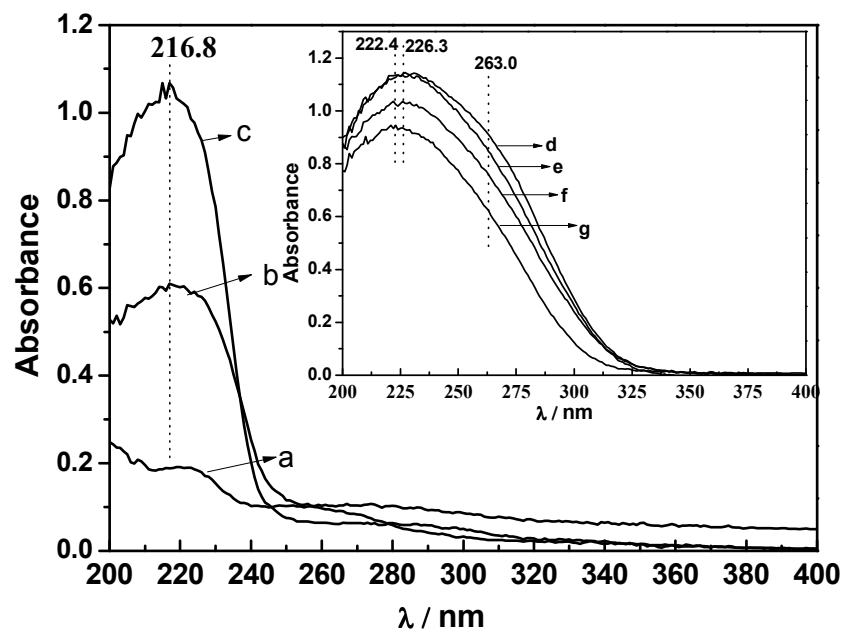
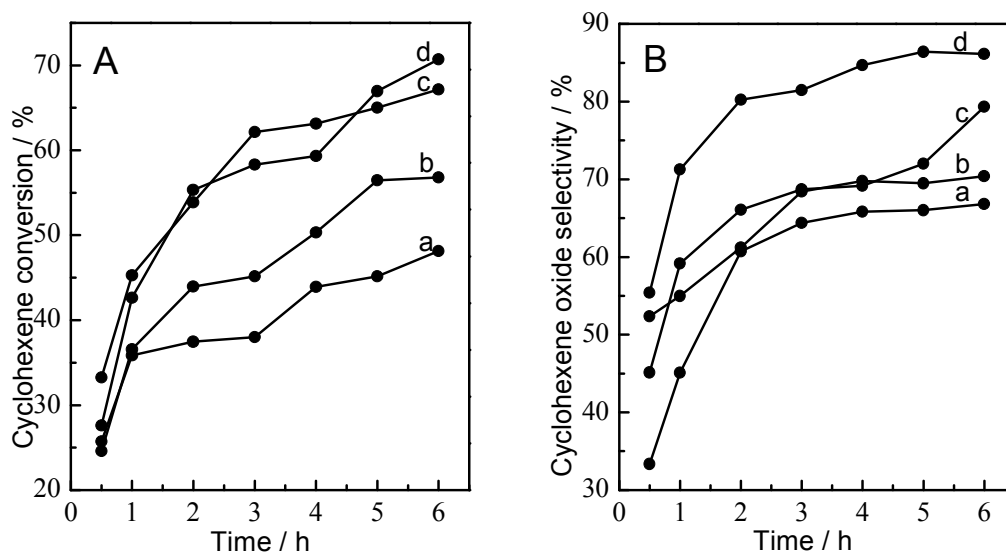
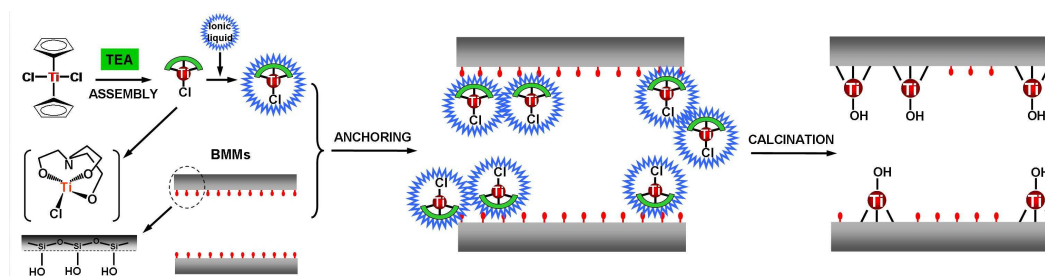


Figure 6.



Scheme 1.



Scheme 1B.

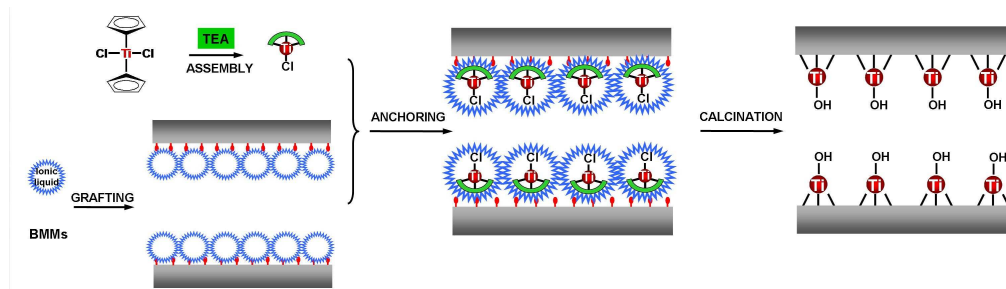


Table 1 Structural parameters and textural properties of all samples

Samples	2θ /°	d_{100} / nm	BET surface area / $\text{m}^2 \cdot \text{g}^{-1}$	Pore volume ^a / $\text{cm}^3 \cdot \text{g}^{-1}$	Small pore size ^b / nm	Large pore size ^b / nm	Ti loading ^c % (wt)	Content of IL ^d / % wt
BMMs	2.11	4.18	980	1.85	2.79	21.02	0	0
ILBMMs	2.17	4.07	601	1.07	2.15	19.69	0	18.0
Ti/BMMs-1	2.34	3.77	878	1.38	2.68	20.50	0.89	16.9
Ti/BMMs-2	2.33	3.78	875	1.42	2.64	20.42	0.89	16.6
Ti/BMMs-3	2.35	3.76	876	1.46	2.64	18.95	1.65	17.0
Ti/BMMs-4	2.34	3.77	865	1.37	2.55	20.61	1.65	17.0

a The total pore volume was determined at the relative pressure of 0.99.

b The mean pore size was calculated from the N₂ desorption branch using the BJH method.

c The results were given by ICP-AES.

d The contents were calculated on the basis of obtained TGA profiles.